Eur Biophys J (2011) 40:259–271
DOI 10.1007/s00249-010-0643-6

ORIGINAL PAPER

The non-native conformations of cytochrome c in sodium dodecyl sulfate and their modulation by ATP

Unnati Ahluwalia · Shahid M. Nayeem · Shashank Deep

Received: 25 August 2010 / Revised: 16 October 2010 / Accepted: 10 November 2010 / Published online: 30 November 2010

Abstract To understand the interaction of cytochrome c (cyt c) with membranes, a systematic investigation of sodium dodecyl sulfate (SDS)-induced conformational alterations in native horse heart ferricytochrome c (pH 7.0) was carried out using heme absorbance, tryptophan fluorescence and circular dichroism (CD) spectroscopy. ATP interaction with membrane-bound cyt c is known to regulate the process of apoptosis. To understand the effect of nucleotide phosphates on membrane-bound cyt c, we also carried out studies of the interaction of ATP with cyt c in the presence of SDS. Fluorescence and UV-Vis data suggest that SDS induces two different transitions (F to C1, C1 to C2) in cyt c, one in the pre-micellar region and the other in the post-micellar region. The fluorescence data further indicated the increase in distance between Trp 59 and heme in the intermediates in both the regions, suggesting loosening up of cyt c on titration with SDS. The far-UV and near-UV CD data suggest partial loss of secondary and tertiary structure in C1, but complete loss of tertiary structure and no further loss of secondary structure in C2. On titration of C1 and C2 with ATP, the secondary structure is restored. However, the heme ligation pattern and heme exposure change only for C2, but not for C1 on the addition of ATP.

Electronic supplementary material The online version of this article (doi:10.1007/s00249-010-0643-6) contains supplementary material, which is available to authorized users.

U. Ahluwalia · S. M. Nayeem · S. Deep (✉)
Department of Chemistry, Indian Institute of Technology, Delhi, India
e-mail: sdeep@chemistry.iitd.ac.in

Keywords Cytochrome c · Sodium dodecyl sulfate · Non-native conformation · ATP · GTP · Docking

Introduction

Cyt c is a protein well known for its electron transport functions in the inner mitochondrial membrane. Membrane-bound cyt c has been observed to have a conformation different from its native state (Pinheiro and Watts 1994; Rytomaa and Kinnunen 1994, 1995; Sinibaldi et al. 2008, 2006, 2003; Spooner and Watts 1991a, b, 1992; Vincent et al. 1987; Vincent and Levin 1986). Studies have suggested a physiological role for the non-native conformation resulting from cyt c binding to membrane (Cortese et al. 1998; Jemmerson et al. 1999). The structural alteration is not only important for electron transfer (Cortese et al. 1998), but also for events like apoptosis (Jemmerson et al. 1999). Therefore, it is important to study the structural properties of membrane-bound cyt c. These considerations have led to a series of studies on cytochrome c in membrane-mimetic systems such as phospholipid vesicles and micelles.

ATP can modulate the electron transfer rate of cyt c with its redox partners by inducing changes in the conformation, ligation, oxidation state as well as stability of the free cyt c (Antalik and Bagel'ova 1995; Craig and Wallace 1991). Similarly, the ratio of ATP/ADP is one of the factors responsible for the cell to undergo apoptosis. Interaction of cyt c with Apaf-1 in the presence of ATP is required for the formation of the apoptosome (Green and Reed 1998). Patriarca et al. (2009) have suggested a physiological role of ATP binding to cyt c at low millimolar concentrations in the cytosol. They proposed that ATP acts as an allosteric effector, regulating structural transitions among different

conformations of cyt c, which are endowed with apoptotic activity or not. Importantly, nucleotide specificity is observed for caspase activation, with the cleavage occurring only in the presence of dATP or ATP (Li et al. 1997; Liu et al. 1996; Sinibaldi et al. 2005).

In the current study, we have investigated the conformational change taking place in cyt c as a result of interaction with SDS. SDS was chosen since it has been widely used as a membrane mimetic. Extensive studies on the interactions of cyt c with SDS have been reported (Bertini et al. 2004; Bhuyan 2010; Chattopadhyay and Mazumdar 2003; Chen et al. 2008; Das et al. 1998; Oellerich et al. 2003; Xu and Keiderling 2004, 2006). However, very little literature providing details about the different non-native conformations of cyt c in the pre- and post-miceller regions is available (Bhuyan 2010; Oellerich et al. 2003). Also, the effect of ATP on the SDS-induced non-native conformations has not been characterized in detail. In this work, the structural characterization of cyt c was carried out through Soret absorbance, equilibrium fluorescence and far- and near-UV CD. The investigations suggest that the SDS induces two different non-native conformations, one in the pre-cmc (C1) and the other in the post-cmc region (C2) with the typical molten globule features. The possible biological role of membrane-bound cyt c in electron transfer and apoptosis is discussed. We also investigated the effect of ATP/GTP on the two non-native conformations induced by SDS. Docking of cyt c with SDS and ATP/GTP was carried out to characterize the putative binding sites of these molecules on cyt c. Information on the docking sites thus obtained was used to explain the experimental data obtained from the binding of cyt c with SDS and the effect of ATP/GTP on the SDS-bound cyt c.

Materials and methods

Horse heart cytochrome c was purchased from Sigma and used as such. Orthophosphoric acid, ATP, GTP, disodium hydrogen phosphate (Na_2HPO_4) and sodium dihydrogen phosphate (NaH_2PO_4) were purchased from SRL (India). HCl and NaOH used to maintain pH were also of analytical reagent grade from SRL. The chemicals were used without further purification. Solutions were prepared in Milli-Q water. The pH was determined on a standard Sartorius (PB-11) pH meter at 25°C.

Stock solutions of cytochrome c were prepared in 70 mM phosphate buffer, pH 7.0, at 25°C. Concentration of protein was measured on a Varian Bio-100 UV-vis spectrophotometer using a molar absorptivity of 106.1 mM^{-1} cm^{-1} at 410 nm. The 1 M nucleotide stocks were made in Milli-Q water and were used in the concentration range of 100 μm^{-1} mM. The nucleotide concentrations were also measured spectroscopically using a molar extinction coefficient of 15,400 $M^{-1}cm^{-1}$ at 260 nm for ATP and molar extinction coefficient of 13,700 M^{-1} cm^{-1} at 253 nm for GTP, at pH 7.

Absorbance spectroscopy

The steady-state UV absorbance of 10 μM cyt c with various concentrations of SDS was recorded at 25°C on a Varian Cary Bio 100. The samples were scanned in the 350–700-nm region to study the effect of SDS on various cyt c-specific bands. The change in steady-state UV-Vis absorbance of cyt c in the presence of sub-micellar (1 mM) or post-micellar concentrations of SDS (>5 mM) was also observed on titration with ATP.

Circular dichroism (CD)

The circular dichroism measurements in the far-UV region (200–250 nm) were performed on Chirascan CD spectrophotometers in 1-mm path length cells at 25°C. To probe the heme environment, CD spectra in the Soret region (350–450 nm) were recorded in a 35-μM cyt c solution in a 5-mm path length cuvette. The Soret CD shows a negative Cotton Soret effect, and its disappearance indicated the breaking up of the Fe-(S) Met bond. All scans were performed on the buffer solution as well and were subtracted from the sample data.

Fluorescence spectroscopy

Fluorescence spectra of cytochrome-c (10 μM) with or without SDS (0–10 mM) were collected on a Varian Cary eclipse fluorescence spectrophotometer with a Peltier-based temperature controller. Excitation and emission wavelengths were kept at 295 and 335 nm, respectively, whereas a slit width of 10 nm (both for excitation and emission) was used for all these experiments.

Peroxidase activity measurement

The peroxidase activity of cyt c (1 μM) alone and in the presence of SDS was measured using hydrogen peroxide and guaicol in 50 mM phosphate at pH 7 and 25°C. Formation of the product tetraguaiacol was followed by measuring absorbance at 470 nm on a Cary 100 UV-Vis spectrophotometer. The concentration of guaiacol and hydrogen peroxide used was 10 and 100 mM, respectively. Peroxidase activity was also measured for cyt c-SDS in the presence of ATP.

Docking simulations

SDS, ATP and GTP were docked on the oxidized horse heart cyt *c* three-dimensional structure (PDB code 1hrc; Bushnell et al. 1990) using the program AutoDock 4.2, which allows docking of flexible ligands on target macromolecules using a Lamarkian genetic algorithm (Morris et al. 1998). In detail, ligands were allowed to explore their conformational space, while the cyt *c* conformation was kept fixed. The blind docking of these ligands was done using a grid size of 62 Å × 62 Å × 62 Å. Docking parameters viz. population size, number of energy evaluations and number of Lamarckian genetic algorithm runs were kept at 250, 25,000,000 and 100, respectively. Autodock default clustering with RMSD 2 Å was used to select the best docked conformation. In most cases, the lowest energy conformation also belongs to the largest cluster. In case of scattered clustering, the lowest energy conformation was selected as the best docked conformation. The procedure yielded 100 different complexes for each ligand, and both the binding-free energy and the ligand intramolecular energy of significant conformation with respect to the existing literature and experimental results were evaluated.

Results

Change in the fluorescence parameters of cyt c on the addition of SDS

Horse cytochrome c has a single tryptophan residue at position 59. The tryptophan fluorescence is quenched in the native state by resonance energy transfer to the heme group. The increase in the tryptophan distance from the heme results in an increase in the fluorescence intensity. Thus, the change in fluorescence intensity is often used as reliable marker of molecular expansion around the heme (Hamada et al. 1993). Figure 1 summarizes the results of fluorescence studies on native cytochrome c at pH 7 in the absence and presence of 0–3 mM SDS. It is evident from the figure that the SDS-induced structural change of cyt c involves at least two transitions, suggesting the presence of at least one intermediate. The first transition (F to C1) was in the submicellar region, resulting in the accumulation of an equilibrium intermediate at ~1 mM SDS concentration, whereas the second transition (C1 to C2) in the post-micellar region resulted in another conformational variant at 3 mM SDS. The cmc of SDS is calculated to be ~1.6 mM in 70 mM phosphate buffer, pH 7.0, at 25°C from the conductivity measurement. The SDS midpoints for the two transitions are 0.5 and 2.5 mM, respectively. Both transitions are accompanied by an increase in fluorescence intensity, indicating an increase in the distance between heme and Trp 59.

The intrinsic fluorescence maximum (λ_{max}) is an excellent parameter to monitor the polarity of the tryptophan environment in protein and is sensitive to the protein conformation (Saini and Deep 2010). The fluorescence increase on the addition of SDS to cyt c is accompanied by a blue shift from 358 to 344 nm. This indicates a more hydrophobic environment around tryptophan. The fluorescence spectrum generally shifts to shorter wavelengths as the polarity of the solvent surrounding the tryptophan residue decreases. The 358-nm emission peak does not shift upon GdnHCl-induced unfolding, suggesting that the environment of Trp in SDS-induced conformation is different from that in the GdnHCl-induced non-native conformation of cyt c.

Change in Soret absorbance of cyt c with the addition of SDS

The Soret band (350–490 nm) is due to the π–π^* transition and report on the spin state/oxidized state of the heme iron. The heme iron in oxidized cyt c is in a low-spin state with two axial ligands provided from His 18 and Met 80. A Soret band with a maximum intensity at 410 nm is typical of the native state of oxidized cyt c, indicative of the presence of both axial ligands. The Soret spectra of cytochrome c (10 μM, pH 7.0) were collected in the presence of SDS and are shown in Fig. 2. λ_{max} decreases with an increase in SDS concentration. The trend of decrease in λ_{max} indicates the presence of two transitions on the addition of SDS, similar to the one observed with fluorescence, one in pre-miceller region and the other in the post-miceller region. During the first transition, λ_{max} decreases from 409 to 407 nm, whereas during the second transition, it decreases from 407 nm to 399 nm. The blue shift for the Soret band is consistent with the disruption of Met-80 ligation to the heme iron. The changes in the Soret band induced by 1 mM SDS at pH 7.0 are akin to those observed for GuHCl or urea-denatured cyt c at pH 7.0 (Babul and Stellwagen 1971; Tsong 1975), whereas changes in the Soret band in the post-miceller region at pH 7.0 are akin to those observed in the presence of 4.5 M GuHCl at pH less than 5 (Colon et al. 1997).

The change in the absorbance of cyt c at 410 nm on titration with SDS (Fig. 3) is also consistent with the earlier data that indicate structural changes in the pre- and post-micellar regions. An increase in the absorbance was observed with the addition of a submicellar concentration of SDS. Surprisingly, the absorbance decreases on the addition of a post-micellar concentration of SDS.

Changes in the Q band are markers for the change in coordination environment of the heme. In the oxidized form,

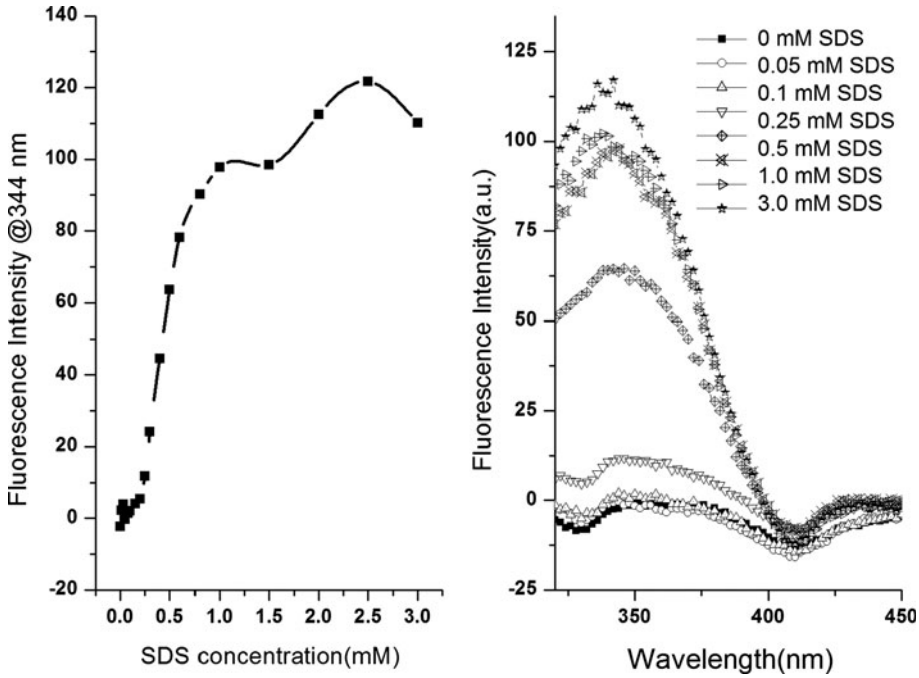

Fig. 1 The fluorescence spectra of 10 μM cyt c in 70 mM phosphate buffer, pH 7.0, in the presence of SDS (*right panel*). The change in intrinsic tryptophan fluorescence intensity of cyt c at 344 nm on the addition of SDS (*left panel*)

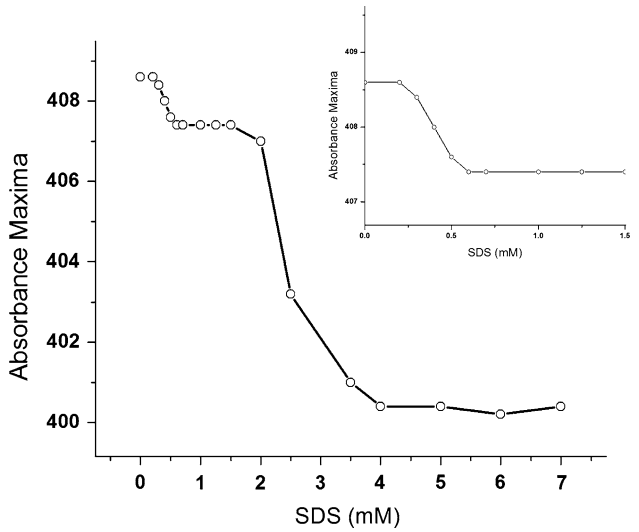

Fig. 2 Change in absorbance maxima of cyt c in 70 mM phosphate buffer, pH 7.0, on the addition of SDS. *Inset* shows the change in absorbance maxima in the pre-cmc region

cyt *c* (between pH 3 and 7) exhibits a low intensity Q band at 528 nm, which is assigned to originate from the 6-coordinated low-spin porphyrin chromophore. Below pH 3, the blue-shifted Q bands at 495 nm are assigned to a 6-coordinated high-spin species (Oellerich et al. 2002). A small blue shift is seen with the addition of SDS (supplementary Fig. 1). The changes in the Q-band induced by SDS at pH 7.0 are similar to those observed in the presence of 9 M urea (Fedurco et al. 2004). The amount of the high-spin species present at pH 7 increases with the addition of SDS.

Change in the far-UV CD spectrum of cyt c on the addition of SDS

CD signal measured at 222 nm is a more selective probe for the helicity because interferences caused by other secondary structure elements are relatively weak at this wavelength. Figure 4 shows the ellipticity value at 222 nm in the presence of varying concentrations of sodium dodecyl sulfate (0–5 mM) at pH value 7. There is a loss of the 222 nm band, indicating the loss of helicity on the addition of SDS up to 2 mM. On the further addition of SDS, no change was observed in far-UV spectra of cyt c. Although there is a loss of the α-helix on the addition of SDS, a large portion of it is retained in SDS-bound cyt c. Interestingly, more prominent changes are observed at 208 nm. These structural changes may arise from the change in contribution of other secondary structural components (Myer 1968).

Change in near-UV CD and Soret CD of cyt c with the addition of SDS

The near-UV CD region (250–330 nm) provides information on the packing of aromatic side chains in the protein. The near-UV CD spectrum of cyt c displays two distinct minima at 282 and 288 nm. These minima have been assigned to tertiary structure packing of Trp 59. Binding of SDS to native cyt c results in a decrease in intensity of these two bands in C1, indicating the partial disruption of the tight packing of core residues in cyt c (Fig. 5, left panel). The disruption is complete in C2.

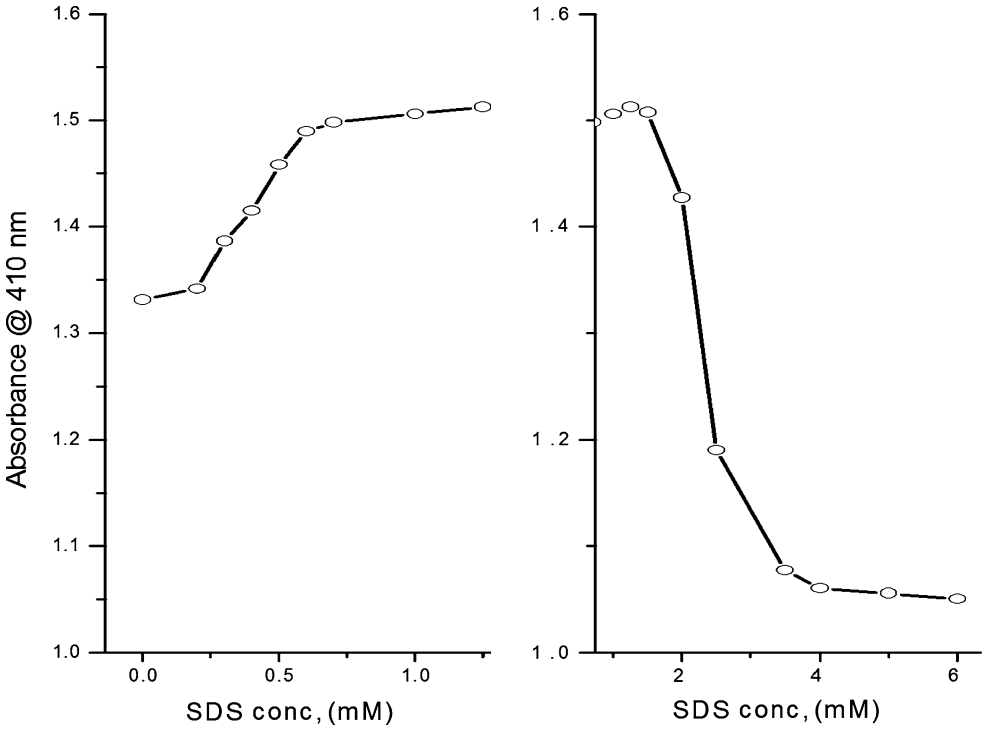

Fig. 3 The Soret absorbance of cyt c at 410 nm on the addition of SDS in the pre-cmc region (*left panel*) and in the post-cmc region (*right panel*)

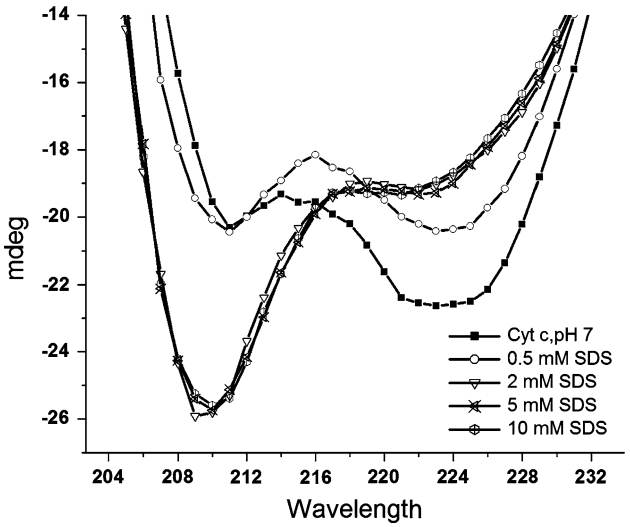

Fig. 4 Far-UV CD of cyt c, pH 7, as a function of SDS concentration

The CD spectrum in the Soret region (350–490 nm) can provide further insight into the integrity of the heme crevice (Myer 1968). The optical activity in this region is generated through the coupling of heme π–π^* electric dipole moments with those of nearby aromatic residues in the protein. The spectrum of cyt c in its native conformation exhibits a strong negative band at about 418 nm and a positive band at 406 nm due to the Cotton Soret effect, primarily a result of heme-polypeptide interactions. In the conformation C1 resulting from the interaction of cyt c with SDS in the pre-cmc region, the Soret CD spectrum is converted to a single positive band with a maximum near 410 nm with the complete loss of the 418-nm CD band (Fig. 5, right panel), identical to that obtained from L-PG micelle binding to native or acid-unfolded cyt c. This type of spectrum is also obtained for urea- or acid-denatured cyt c, and has been observed for cyt c bound to DOPS vesicles. The Soret spectral changes indicate that the coupling between the heme π–π^* transitions and those of the aromatic residues nearby have been disrupted upon binding of native cyt c to SDS. There is no change of the 418-nm band on further addition of SDS in the post-cmc region.

Change in the peroxidase activity of cyt c in the presence of SDS

The guaiacol assay can be used to estimate the compactness of the cyt c intermediates, heme penetration by small molecules like H_2O_2 and peroxidase activity. Figure 6 shows the absorbance of tetra-guaiacol at 470 nm in the presence of SDS. The figure indicates that SDS induces a peroxidase activity increase in cyt c. It also indicates that the peroxidase activity of C2 is higher than that of C1.

Effect of salt on the cyt c-SDS interaction

Figure 7 shows the effect of salt (NaCl) on the conformational transitions of cyt c in the presence of SDS. It is evident that NaCl affects the second transition, but not the

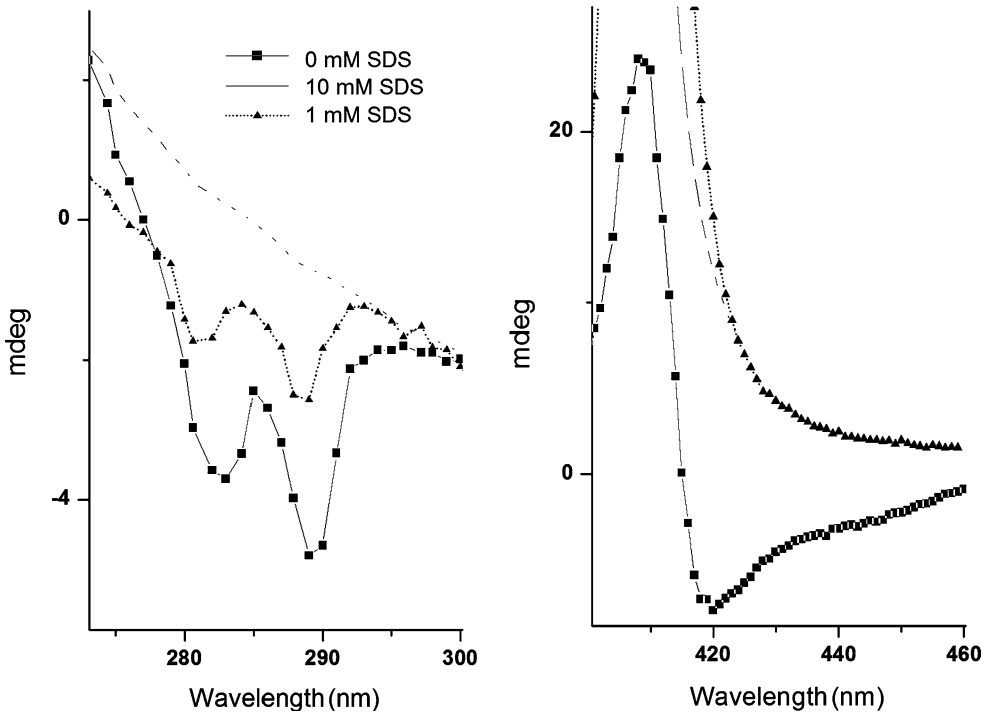

Fig. 5 Change in the near-UV CD (*left panel*) and Soret CD band (*right panel*) of cyt c on the addition of SDS

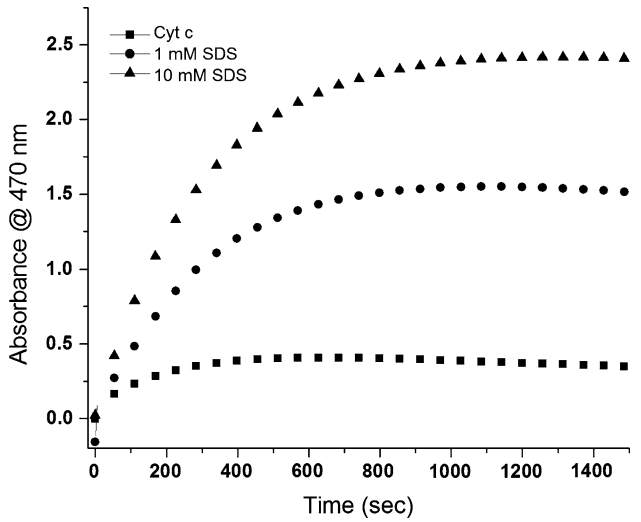

Fig. 6 Peroxidase activity of cyt c, as measured as absorbance of tetra guaiacol at 470 nm, as a function of time in the presence of SDS

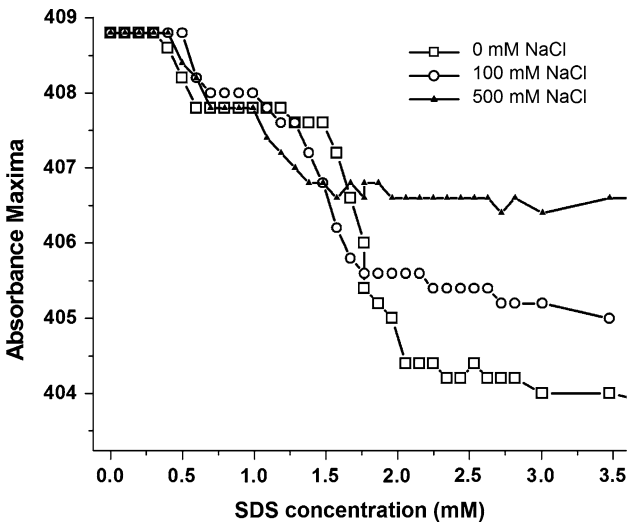

Fig. 7 Effect of NaCl on transitions of cyt c (pH 7.0, 70 mM phosphate buffer) induced by SDS

first. C1 to C2 takes place at lower concentrations of SDS. The wavelength maxima of C2 also changes with the addition of NaCl. There is a red shift indicating the decrease in the amount of high-spin species. The cmc of SDS in 70 mM phosphate buffer decreases to 1.4 and 0.4 mM in the presence of 100 mM NaCl and 500 mM NaCl, respectively. The cmc values are consistent with the reported values in the literature (Umlong and Ismail 2007).

Change in Soret absorbance of C1/C2 on the addition of ATP

Figure 8 shows the effect of ATP on the Soret spectra of cyt c in the presence of SDS. The Soret absorbance maxima of C1 does not show any change on the addition of ATP. However, there is a blue shift of absorbance maxima on the addition of ATP to C2 along with a decrease in

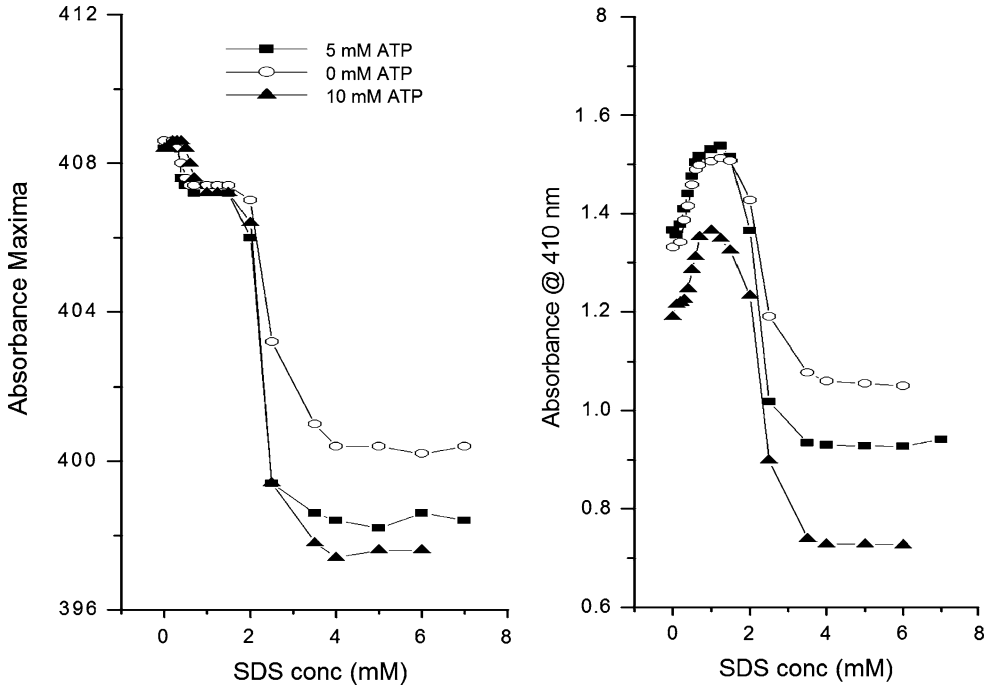

Fig. 8 Effect of the addition of SDS on absorbance maxima and absorbance of cyt c (70 mM phosphate buffer, pH 7) in absence/presence of ATP

absorbance at 410 nm. The Q-band of C2 also shows a blue shift on the addition of ATP (Supplementary Fig. 2).

Change in CD spectra of the cyt c-SDS system on the addition of ATP

To see the effect of ATP on the secondary stucture of conformations C1 and C2 of cyt c resulting from the addition of SDS, the far-UV CD spectra were recorded for C1 (cyt c + 1 mM SDS, Fig. 9) and C2 (cyt c + 10 mM SDS, Fig. 10), respectively, in the presence of ATP. It is evident that there is a recovery of the 222 nm band on the addition of ATP in both conformations. Figure 9b shows the ellipticity of C1 at 222 nm as a function of temperature in the absence/presence of ATP. The ellipticity of C1 is larger in the presence of ATP at every temperature. However, on the addition of GTP, there is no recovery of the 222-nm band on the addition of GTP (supplementary Fig. 3).

To see the effect of ATP/GTP on the tertiary structure and the heme environment, the near-UV CD and Soret CD were also recorded for cyt c + 1 mM SDS and cyt c + 10 mM SDS, respectively, in the presence of GTP (figure not shown). The addition of ATP/GTP had a negligible effect on the near-UV and Soret band of conformations C1 and C2.

Peroxidase activity of C1/C2 in the presence of ATP

The peroxidase activity of C1 and C2 was measured as the absorbance of tetra-guaiacol at 470 nm in the presence of ATP (supplementary Fig. 4). The figure indicates that there is no significant change in the peroxidase activity of C1 on the addition of ATP. However, a decrease in peroxidase activity was observed for C2.

Docking of cyt c with SDS

SDS was docked on cyt c using Autodock. Figure 11 shows the putative cyt c-SDS complex obtained on docking. Several specific interactions between SDS and cyt c can be observed. There is a strong electrostatic interaction between the sulfate group of SDS and Lys87 and 88 of cyt c, whereas hydrophobic interactions are present between the hydrophobic chain of SDS and Glu62, Glu66, Met65 and Arg91. The calculated binding energy for the complex formation at this site is −4.43 kcal/mol, equivalent to a binding constant (Kd) of 5.63×10^{-4} M.

Docking of cyt c with ATP and GTP

Cyt c was docked with ATP using Autodock to examine the potential binding site of ATP on cyt c. The lowest energy structure thus obtained is shown in Fig. 12. As indicated by the figure, the ATP binds to the site near the exposed heme. A closer look at this docked structure shows a strong electrostatic interaction between the phosphate oxygen of ATP and e-NH2 of Lys72 and amide nitrogen of Phe82. Other electrostatic interactions present are between the adenine moiety of ATP and carboxyl oxygen of Gly84, and between the ribose moeity of ATP and amide nitrogen of Ala83. The hydrophobic interaction is predicted between

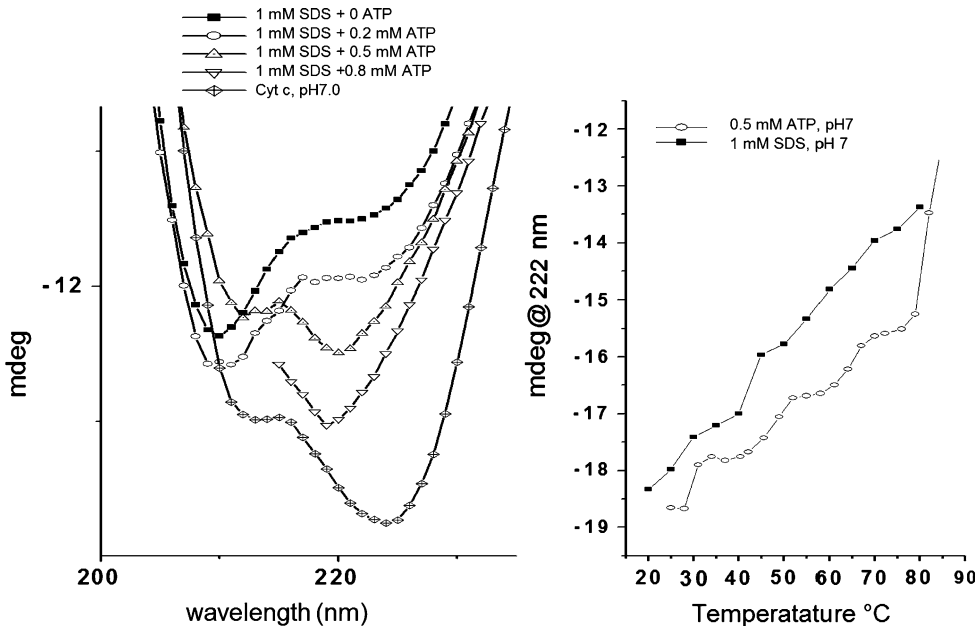

Fig. 9 The far-UV CD of C1 (cyt c with 1 mM SDS) in the presence of different concentrations of ATP (*left panel*). The change in ellipticity of C1 alone and in the presence of 0.5 mM ATP at 222 nm as a function of temperature (*right panel*)

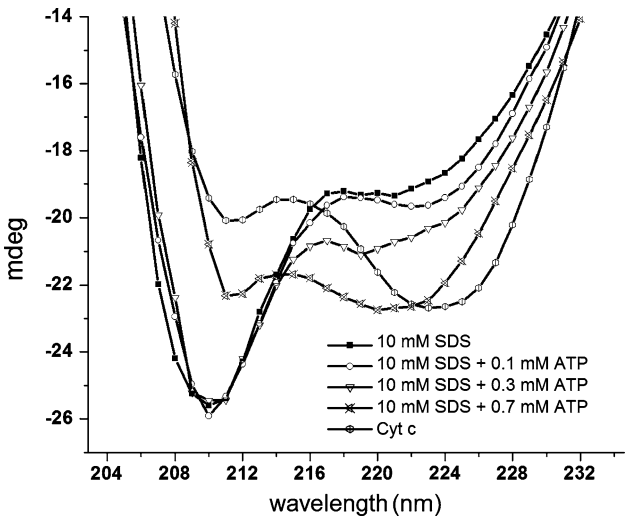

Fig. 10 The far-UV CD of C2 (cyt c with 10 mM SDS) in the presence of different concentrations of ATP

Gln16 and heme 105 of cyt c with ATP. The calculated binding energy for the complex formation is −7.68 kcal/mol, equivalent to a binding constant (Kd) of 2.34×10^{-6} M.

Another important docked structure is given in Fig. 13. This structure predicts the electrostatic interaction between the phosphate group of ATP and Lys87 and Lys88 of cyt c. Other important interactions are electrostatic interactions between Glu 62, Glu 69 and Arg91 and the adenine moiety of ATP. The binding energy of the docked structure was calculated to be −6.07 kcal/mol.

There was a third cluster of docked structures seen around residues Val20-Lys27 of cyt c (supplemetary Fig. 5). Electrostatic interactions are observed between the phosphate of ATP and Lys25, Lys27 of cyt c. Other important interactions present in this structure are the hydrophobic interaction of Ala15, Val20, Phe10, Glu21 of cyt c and ATP. The binding energy of this structure was calculated to be −5.8 kcal/mol.

Cyt c was also docked with GTP to examine the potential interaction site of cyt c with GTP. An electrostatic interaction exists between the phosphate of GTP and Lys25 of cyt c, Glu21 and Lys25 of cyt c and the sugar moeity of GTP; a hydrophobic interaction exists between Lys27 and the G moeity (supplemetary Fig. 6). The calculated binding constant was −5.96 kcal/mol, equivalent to a binding constant (Kd) of 4.28×10^{-5} M.

Another important site for GTP binding is the same site that is involved in the lowest energy cyt c-ATP complex. In this conformation, an electrostatic interaction of Lys72, Glu69, Ala83 and a hydrophobic interaction with Gly84 and Lys86 exist with GTP (Supplementary Fig. 7). The binding energy of GTP at this site is −3.89, equivalent to a binding constant (Kd) of 1.4×10^{-6} M. It is worthwhile to note that the binding energy of ATP (−7.68 kcal/mole) is considerably higher than that for cyt c- GTP complex for this site.

Discussion

SDS induces the unfolding of cyt c. According to the sequential model proposed by Englander and co-workers (Bai et al. 1995), cyt c unfolds and refolds by a pathway consisting of the same number of intermediates, stabilized

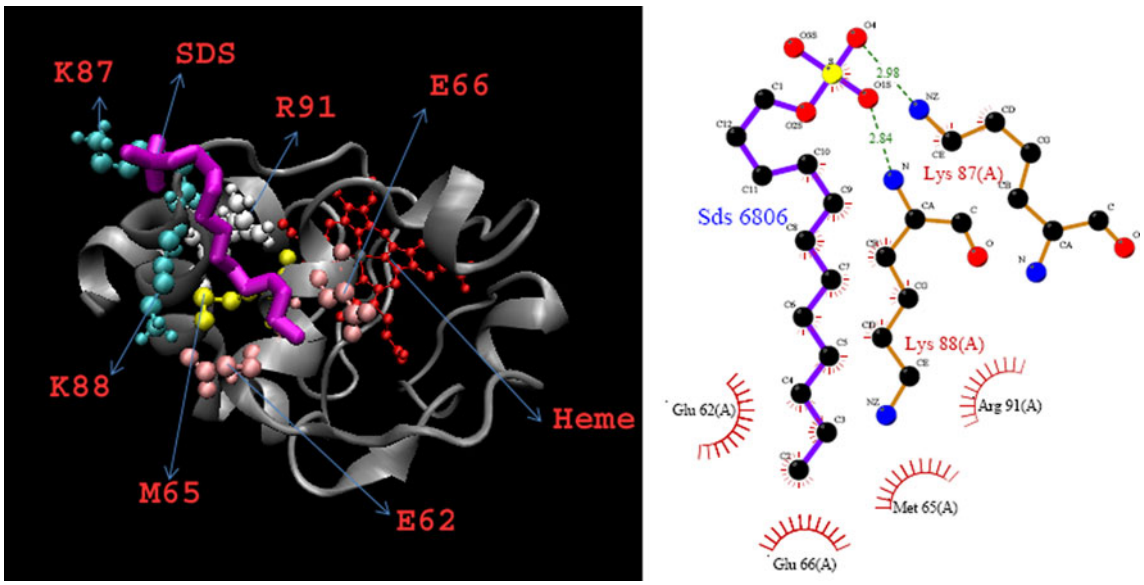

Fig. 11 The putative binding site of SDS on cyt c as obtained from docking of SDS on cyt c using Autodock (*left panel*). The *right panel* depicts the different hydrophobic and electrostatic interactions between SDS and cyt c as obtained from ligplot

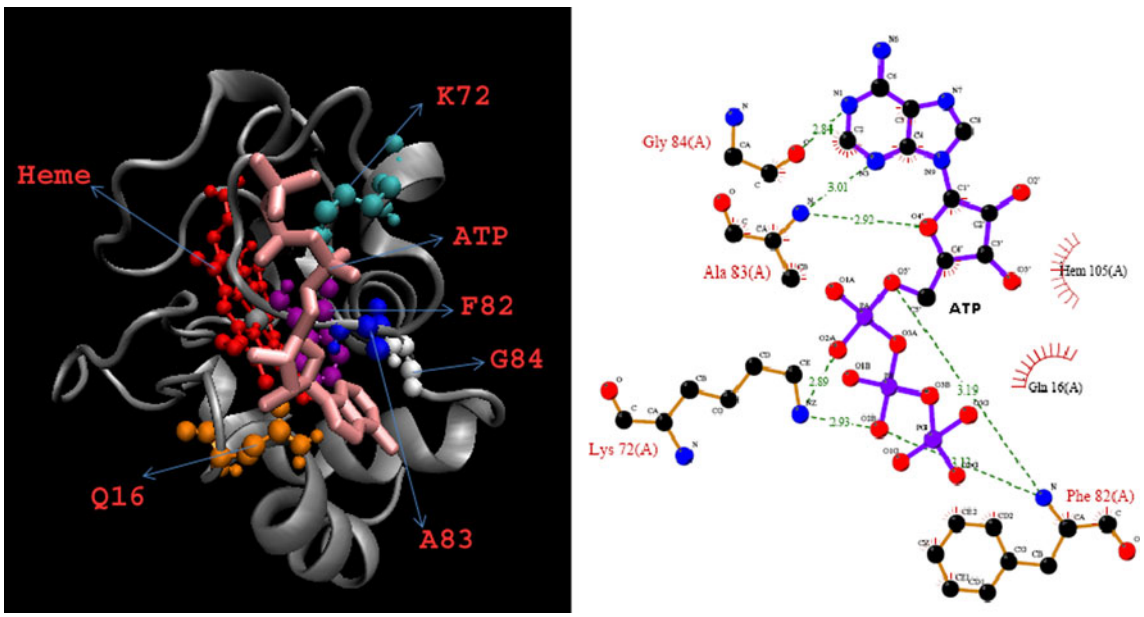

Fig. 12 Putative binding site of ATP on cyt c obtained using Autodock (*left panel*). The *right panel* depicts the different hydrophobic and electrostatic interactions between SDS and cyt c as obtained from ligplot

by step-by-step folding of cooperative units. As cooperative units, the model describes five main segments: (1) the loop formed by residues 70–85 (F1), (2) the loop formed by residues 36–61 (F2), (3) the 20–35 loop and 60's helix (residue 60–70) (F3), and (4) the amino-terminal helix (residue 2–15) and carboxy-terminal helix (residue 87–104) in the order of unfolding energy (F4).

The UV-Vis and fluorescence data of cyt c titration with SDS indicate that the SDS-induced unfolding of cyt c follows a biphasic mechanism. On the addition of a submicellar concentration of SDS, the protein (F) unfolds to an intermediate conformation (C1). On further addition of SDS in the post-cmc region, this intermediate form unfolds further to give another conformation (C2). This suggests two distinct modes of SDS interaction with cyt c. The first phase transition is due to the structural change induced by the SDS monomer, whereas the second transition is due to structural changes induced by SDS micelles. The absence of the characteristic CD band in the Soret region for SDS-induced intermediates indicates the lack of

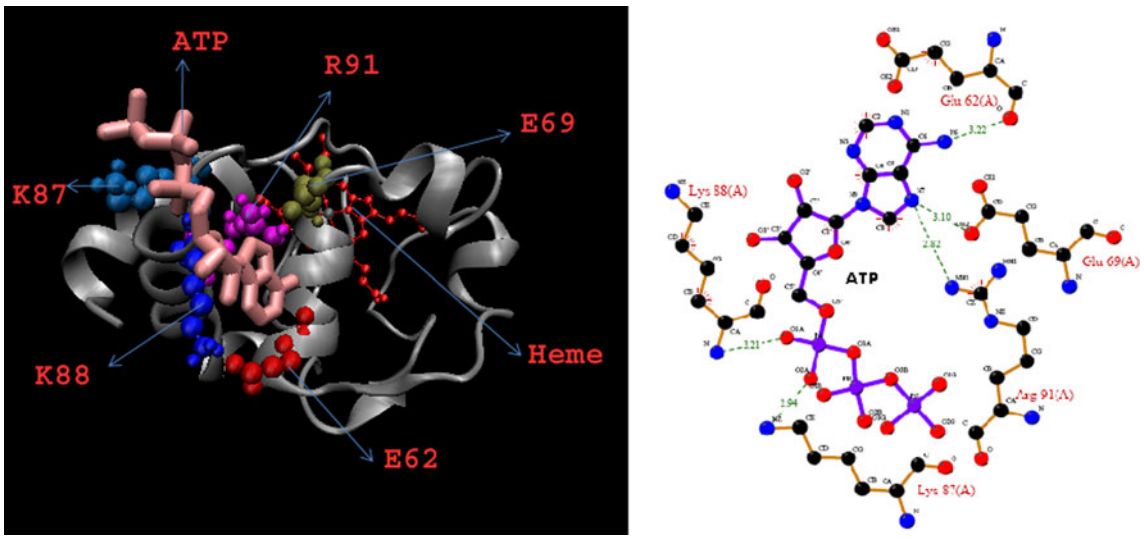

Fig. 13 Second important putative binding site for ATP on cyt c (*left panel*). Important interactions in this docked structure are shown in the *right panel*

tertiary interactions in segment 70–85 and the rupture of Met80-heme coordination. UV-Vis data are also consistent with the rupture of the Met80-Fe(III) axial bond. The observed conformational transition is consistent with unfolding of the lowest cooperative unit F1, consisting of the 70–85 loop. This is typical of the A-state of cyt c (Goto et al. 1990; Jeng et al. 1990; Jordan et al. 1995), in which only His 18 of two native axial ligands remained coordinated to the heme iron. The change in absorption lambda max from 409 to 407 nm indicates that the C1 is a low-spin Fe(III)-heme intermediate formed probably due to misligation with histidine. Loss of the near-UV CD band around 285 nm suggests the loss of well-defined conformation in loops formed by residues 36–61. Fluorescence data indicate an expanded Trp59-heme distance and are consistent with changes in this loop. Unfolding of loops formed by 36–61 is not surprising since this is the cooperative folding unit with the second lowest folding energy. Far-UV SDS titration data in the pre-cmc region indicate the partial loss of the secondary structure. This indicates a partial unfolding of the third cooperative unit, which is formed by three helical segments. On the whole, the experiments described here suggest that SDS-bound cyt *c* is likely to have a disrupted Met80-heme ligation, an expanded Trp59-heme distance and retention of a major portion of the α-helical structure, all features characteristic of the molten globule state of cyt *c*. Godoy et al. (2009) reported that a variant of cyt c, M80A-cytc, has increased peroxidase activity and is spontaneously released from mitochondria, translocating to the cytoplasm and the nucleus. This finding suggests the possibility that protein structural alterations that disrupt the M80-Fe ligation stimulate nuclear translocation and confer new functions to cyt c in nonapoptotic cells. F to C1 transition was not affected on the addition of NaCl, suggesting that the interaction of cyt c with submicellar concentrations of SDS is predominantly hydrophobic.

The occurrence of the second transition at SDS concentrations higher than the critical micelle concentration (cmc) suggests a different mode of binding for SDS. Fluorescence and peroxidase data suggest the further expansion of cyt c, whereas far-UV CD data suggest no loss of secondary structure in going from C1 to C2. The presence of an appreciable amount of secondary structure indicates that the C2 is not completely unfolded. Near-UV CD data suggest a complete loss of tertiary structure. Absorption λ_{max} changes from 407 to 400 nm. This transition is similar to the change observed for GuHCl denatured cyt c on lowering the pH (Colon et al. 1997). The transition, in this case, was assigned to the loss of strong field ligand coupled with the protonation of side chain nitrogen. Thus, C2 is probably a high-spin 5-coordinated Fe(III)-heme intermediate. Addition of NaCl affects the second transition, suggesting the predominant role of electrostatic interaction. NaCl may affect this transition by either reducing the cmc of SDS or by interfering with the interaction of cyt c with SDS. Only in the presence of bound micelles high-spin species are formed, confirming the importance of electrostatic interaction in binding of SDS micelles to cyt c.

The denaturation of cyt c that occurs due to the disruption of the mitochondrial membrane may result in a molten globule type conformation, as suggested by many studies. MG conformation of cyt c can be induced at low or high pH, in the presence of a suitable concentration of guanidine hydrochloride and urea, at high temperatures,

and in the presence of sugars, alcohols, polyanions such as poly(vinylsulfate), membrane mimetics such as phospholipids and oleic acid, and *n*-alkyl sulfates (Das et al. 1998; Davis-Searles et al. 1998; Moza et al. 2006; Pinheiro et al. 1997; Sanghera and Pinheiro 2000; Sedlak and Antalik 1999).

Our docking studies of cyt c with SDS indicate the involvement of the residues in the 60's helix (Glu 62, Glu 66 and Met 74) and others like Lys 87, Lys 88 and Arg 99 in cyt c. The Glu-66-Tyr-74 salt link is important for the stability of the loop containing 70–85 segment, whereas Glu-62 to Lys-60 ion pair interaction is important for the stability of the 36–61 loop. The unfolding of these segments has been observed in case of Glu-66-Gly and Glu-62-Gly variants of cyt c, respectively (Maity et al. 2005). Thus, it is not surprising to expect that the hydrophobic binding of monomeric SDS to cyt *c* in this region destabilizes the 70–85 residue poly-peptide segment by breaking the salt link, promoting the weakening or rupture of the Met80-Fe(III) axial bond. It is also expected to destabilize the 36–61 loop, which contains Trp 59. The loss of secondary structure is also not surprising since a significant portion of the 60's helix is involved in binding with SDS.

Cyt *c* interacts with APAF-1, dATP, or ATP and procaspase in the cytosol to form an apoptosome; thus, there must be a mechanism for cyt *c* translocation to cytosolic states. Keeping this in mind, we investigated the interaction of SDS-bound ferricyt *c* with nucleotides. Although ATP was not able to bring back ligand coordination of heme, far-UV CD, electronic absorption demonstrates that the lost secondary structure upon binding of cyt *c* to SDS was regained on the addition of ATP at millimolar concentrations. Furthermore, ATP, but not GTP, is effective in completely restoring the secondary structure of C1/C2 at millimolar concentration.

Docking of cyt c with ATP suggests two different putative binding sites for ATP: (1) a site consisting of residues 82–84; (2) a site consisting of residues Lys87, Lys88, Glu62, Glu69 and Arg91. The residues involved in the second site are similar to the one that was involved in the binding with SDS, the exception being Glu66. ATP was able to mitigate the destabilizing nature of SDS by competing for the same binding site, and thus, the stability of 60's helix and the loop 36-61 was regained. However, the loop 70–85 is still unfolded since ATP does not have a tendency to bind Glu69. It has been reported that cyt *c* from the yeast *Saccharomyces cerevisiae* lacks pro-apoptotic activity (Kluck et al. 2000). Glu62 and Lys88 in horse cyt c are replaced by Asn and Glu in cyt *c* from the yeast *Saccharomyces cerevisia*, respectively. Sinibaldi et al. (2005) showed that the yeast cyt c double mutant, Asn62Glu/Glu88Lys, interacts with ATP, whereas the wild type does not, confirming the importance of such residues in the binding of ATP.

In addition, docking simulations suggest a further explanation for the capacity of ATP, but not GTP, to restore the lost secondary structure of cyt c due to its interaction with SDS. The two lowest docked structures reveal the lack of interaction between Glu62 and GTP, in contrast to its interaction with ATP. Thus, the conclusions of the spectroscopic studies and the ATP, GTP docking simulations are in full agreement, revealing that cyt *c* has a much greater affinity for ATP than GTP.

Several reports are available in the literature in which the interaction between cyt c and SDS has been investigated as discussed in the Introduction section. Bertini et.al. (2004) looked at the axial ligation state of cyt c in the presence of 100 mM SDS through NMR, whereas Chen et al. (2008) investigated the folding kinetics of the SDS-induced molten globule of cyt c. Chattopadhyay et al. (2003) and Das et al. (1998) investigated cyt c structure and stability in the presence of submicellar concentrations of SDS. As observed during our investigation, a partial loss of secondary structure was seen. However, a comparative study of structural changes in the pre- and post-micellar regions was not carried out. Bhuyan (2010) investigated the changes in ferro-cyt c on the addition of SDS in both pre- and post-cmc regions. Only Ollerich et al. (2003) investigated the changes in ferri-cyt c on the addition of SDS in the pre- and post-miceller regions. However, several aspects of SDS interaction with cyt c were not fully explored, such as at which concentration of SDS the transitions took place and what is the effect of ionic strength on the mid-point transition? We predicted the putative binding site of SDS on cyt c based on docking and postulated how this binding affects the different sub-domains of cyt c. Also an important biological question, the apoptotic activity of the resultant conformation, was not studied. One of the important aspects of our study is how ATP affects the different transitions of cyt c. It was found that ATP is able to restore the secondary structure of SDS-bound cyt c. None of the previous studies looked at the interaction of ATP with SDS-induced conformation in cyt c.

Conclusions

In summary, experimental data suggest that SDS induces two different non-native conformations, C1 and C2, in cyt c. C1 results from the interaction of SDS monomer with cyt c, whereas C2 results from the interaction of SDS micelle with cyt c. The extent of the secondary structure, tertiary structure, compactness and environment of heme is different for C1/C2 and native cyt c. C1 and C2 have features of a molten globule. They have a similar secondary

structure and spin state, but a different amount of tertiary structure and different ligation state of heme. The interaction studies of C1 and C2 with ATP indicate that the lost secondary structure of cyt c in C1 and C2 is regained. However, the recovery is not evident on the addition of GTP to C1 or C2. Docking studies indicate that ATP competes for the same site where SDS is supposed to bind, thus displacing SDS and stabilizing cyt c.

Acknowledgments This work was generously supported by the Department of Science and Technology (DST), Government of India, and the Council of Scientific and Industrial Research (CSIR), Government of India, through grants to S.D. U.A. would like to thank CSIR, Government of India, for a fellowship. We acknowledge the use of the advanced instrumentation facility provided by Jawaharlal Nehru University, Delhi, for carrying out CD measurements.

References

Antalik M, Bagel'ova J (1995) Effect of nucleotides on thermal stability of ferricytochrome C. Gen Physiol Biophys 14:19–37

Babul J, Stellwagen E (1971) The existence of heme-protein coordinate-covalent bonds in denaturing solvents. Biopolymers 10:2359–2361

Bai Y, Sosnick TR, Mayne L, Englander SW (1995) Protein folding intermediates: native-state hydrogen exchange. Science 269: 192–197

Bertini I, Turano P, Vasos PR, Bondon A, Chevance S, Simonneaux G (2004) Cytochrome c and SDS: a molten globule protein with altered axial ligation. J Mol Biol 336:489–496

Bhuyan AK (2010) On the mechanism of SDS-induced protein denaturation. Biopolymers 93:186–199

Bushnell GW, Louie GV, Brayer GD (1990) High-resolution three-dimensional structure of horse heart cytochrome c. J Mol Biol 214:585–595

Chattopadhyay K, Mazumdar S (2003) Stabilization of partially folded states of cytochrome c in aqueous surfactant: effects of ionic and hydrophobic interactions. Biochemistry 42:14606–14613

Chen E, Van Vranken V, Kliger DS (2008) The folding kinetics of the SDS-induced molten globule form of reduced cytochrome c. Biochemistry 47:5450–5459

Colon W, Wakem LP, Sherman F, Roder H (1997) Identification of the predominant non-native histidine ligand in unfolded cytochrome c. Biochemistry 36:12535–12541

Cortese JD, Voglino AL, Hackenbrock CR (1998) Multiple conformations of physiological membrane-bound cytochrome c. Biochemistry 37:6402–6409

Craig DB, Wallace CJ (1991) The specificity and Kd at physiological ionic strength of an ATP-binding site on cytochrome c suit it to a regulatory role. Biochem J 279(Pt 3):781–786

Das TK, Mazumdar S, Mitra S (1998) Characterization of a partially unfolded structure of cytochrome c induced by sodium dodecyl sulphate and the kinetics of its refolding. Eur J Biochem 254:662–670

Davis-Searles PR, Morar AS, Saunders AJ, Erie DA, Pielak GJ (1998) Sugar-induced molten-globule model. Biochemistry 37:17048–17053

Fedurco M, Augustynski J, Indiani C, Smulevich G, Antalik M, Bano M, Sedlak E, Glascock MC, Dawson JH (2004) The heme iron coordination of unfolded ferric and ferrous cytochrome c in neutral and acidic urea solutions. Spectroscopic and electrochemical studies. Biochim Biophys Acta 1703:31–41

Godoy LC, Munoz-Pinedo C, Castro L, Cardaci S, Schonhoff CM, King M, Tortora V, Marin M, Miao Q, Jiang JF, Kapralov A, Jemmerson R, Silkstone GG, Patel JN, Evans JE, Wilson MT, Green DR, Kagan VE, Radi R, Mannick JB (2009) Disruption of the M80-Fe ligation stimulates the translocation of cytochrome c to the cytoplasm and nucleus in nonapoptotic cells. Proc Natl Acad Sci USA 106:2653–2658

Goto Y, Calciano LJ, Fink AL (1990) Acid-induced folding of proteins. Proc Natl Acad Sci USA 87:573–577

Green DR, Reed JC (1998) Mitochondria and apoptosis. Science 281:1309–1312

Hamada D, Hoshino M, Kataoka M, Fink AL, Goto Y (1993) Intermediate conformational states of apocytochrome c. Biochemistry 32:10351–10358

Jemmerson R, Liu J, Hausauer D, Lam KP, Mondino A, Nelson RD (1999) A conformational change in cytochrome c of apoptotic and necrotic cells is detected by monoclonal antibody binding and mimicked by association of the native antigen with synthetic phospholipid vesicles. Biochemistry 38:3599–3609

Jeng MF, Englander SW, Elove GA, Wand AJ, Roder H (1990) Structural description of acid-denatured cytochrome c by hydrogen exchange and 2D NMR. Biochemistry 29:10433–10437

Jordan T, Eads JC, Spiro TG (1995) Secondary and tertiary structure of the A-state of cytochrome c from resonance Raman spectroscopy. Protein Sci 4:716–728

Kluck RM, Ellerby LM, Ellerby HM, Naiem S, Yaffe MP, Margoliash E, Bredesen D, Mauk AG, Sherman F, Newmeyer DD (2000) Determinants of cytochrome c pro-apoptotic activity. The role of lysine 72 trimethylation. J Biol Chem 275:16127–16133

Li P, Nijhawan D, Budihardjo I, Srinivasula SM, Ahmad M, Alnemri ES, Wang X (1997) Cytochrome c and dATP-dependent formation of Apaf-1/caspase-9 complex initiates an apoptotic protease cascade. Cell 91:479–489

Liu X, Kim CN, Yang J, Jemmerson R, Wang X (1996) Induction of apoptotic program in cell-free extracts: requirement for dATP and cytochrome c. Cell 86:147–157

Maity H, Maity M, Krishna MM, Mayne L, Englander SW (2005) Protein folding: the stepwise assembly of foldon units. Proc Natl Acad Sci USA 102:4741–4746

Morris GM, Goodsell DS, Halliday RS, Huey R, Hart WE, Belew RK, Olson AJ (1998) Automated docking using a Lamarckian genetic algorithm and an empirical binding free energy function. J Comput Chem 19:1639–1662

Moza B, Qureshi SH, Islam A, Singh R, Anjum F, Moosavi-Movahedi AA, Ahmad F (2006) A unique molten globule state occurs during unfolding of cytochrome c by LiClO4 near physiological pH and temperature: structural and thermodynamic characterization. Biochemistry 45:4695–4702

Myer YP (1968) Far ultraviolet circular dichroism spectra of cytochrome c. Biochim Biophys Acta 154:84–90

Oellerich S, Wackerbarth H, Hildebrandt P (2002) Spectroscopic characterization of nonnative conformational states of cytochrome c. J Phys Chem B 106:6566–6580

Oellerich S, Wackerbarth H, Hildebrandt P (2003) Conformational equilibria and dynamics of cytochrome c induced by binding of sodium dodecyl sulfate monomers and micelles. Eur Biophys J 32:599–613

Patriarca A, Eliseo T, Sinibaldi F, Piro MC, Melis R, Paci M, Cicero DO, Polticelli F, Santucci R, Fiorucci L (2009) ATP acts as a regulatory effector in modulating structural transitions of cytochrome c: implications for apoptotic activity. Biochemistry 48:3279–3287

Pinheiro TJ, Watts A (1994) Lipid specificity in the interaction of cytochrome c with anionic phospholipid bilayers revealed by solid-state 31P NMR. Biochemistry 33:2451–2458

Pinheiro TJ, Elove GA, Watts A, Roder H (1997) Structural and kinetic description of cytochrome c unfolding induced by the interaction with lipid vesicles. Biochemistry 36:13122–13132

Rytomaa M, Kinnunen PK (1994) Evidence for two distinct acidic phospholipid-binding sites in cytochrome c. J Biol Chem 269:1770–1774

Rytomaa M, Kinnunen PK (1995) Reversibility of the binding of cytochrome c to liposomes. Implications for lipid-protein interactions. J Biol Chem 270:3197–3202

Saini K, Deep S (2010) Relationship between the wavelength maximum of a protein and the temperature dependence of its intrinsic tryptophan fluorescence intensity. Eur Biophys J 39:1445–1451

Sanghera N, Pinheiro TJ (2000) Unfolding and refolding of cytochrome c driven by the interaction with lipid micelles. Protein Sci 9:1194–1202

Sedlak E, Antalik M (1999) Molten globule-like state of cytochrome c induced by polyanion poly(vinylsulfate) in slightly acidic pH. Biochim Biophys Acta 1434:347–355

Sinibaldi F, Piro MC, Howes BD, Smulevich G, Ascoli F, Santucci R (2003) Rupture of the hydrogen bond linking two Omega-loops induces the molten globule state at neutral pH in cytochrome c. Biochemistry 42:7604–7610

Sinibaldi F, Mei G, Polticelli F, Piro MC, Howes BD, Smulevich G, Santucci R, Ascoli F, Fiorucci L (2005) ATP specifically drives refolding of non-native conformations of cytochrome c. Protein Sci 14:1049–1058

Sinibaldi F, Howes BD, Piro MC, Caroppi P, Mei G, Ascoli F, Smulevich G, Santucci R (2006) Insights into the role of the histidines in the structure and stability of cytochrome c. J Biol Inorg Chem 11:52–62

Sinibaldi F, Fiorucci L, Patriarca A, Lauceri R, Ferri T, Coletta M, Santucci R (2008) Insights into cytochrome c-cardiolipin interaction. Role played by ionic strength. Biochemistry 47:6928–6935

Spooner PJ, Watts A (1991a) Reversible unfolding of cytochrome c upon interaction with cardiolipin bilayers. 1. Evidence from deuterium NMR measurements. Biochemistry 30:3871–3879

Spooner PJ, Watts A (1991b) Reversible unfolding of cytochrome c upon interaction with cardiolipin bilayers. 2. Evidence from phosphorus-31 NMR measurements. Biochemistry 30:3880–3885

Spooner PJ, Watts A (1992) Cytochrome c interactions with cardiolipin in bilayers: a multinuclear magic-angle spinning NMR study. Biochemistry 31:10129–10138

Tsong TY (1975) An acid induced conformational transition of denatured cytochrome c in urea and guanidine hydrochloride solutions. Biochemistry 14:1542–1547

Umlong IM, Ismail K (2007) Micellization behaviour of sodium dodecyl sulfate in different electrolyte media. Colloids Surf A Physicochem Eng Asp 299:8–14

Vincent JS, Levin IW (1986) Interaction of Ferricytochrome-C with Cardiolipin Multilayers - a Resonance Raman-Study. J Am Chem Soc 108:3551–3554

Vincent JS, Kon H, Levin IW (1987) Low-temperature electron paramagnetic resonance study of the ferricytochrome c-cardiolipin complex. Biochemistry 26:2312–2314

Xu Q, Keiderling TA (2004) Effect of sodium dodecyl sulfate on folding and thermal stability of acid-denatured cytochrome c: a spectroscopic approach. Protein Sci 13:2949–2959

Xu Q, Keiderling TA (2006) Stop-flow kinetics studies of the interaction of surfactant, sodium dodecyl sulfate, with acid-denatured cytochrome c. Proteins 63:571–580